European Journal of Applied Sciences – Vol. 11, No. 3
Publication Date: June 25, 2023
DOI:10.14738/aivp.113.14932
Smulsky, J. J. **(**2023). Neutrino is the Brightest Particle of the Fictitious Micro-world. European Journal of Applied Sciences, Vol - 11(3). 616-633.

Neutrino is the Brightest Particle of the Fictitious Micro-world

Joseph J. Smulsky
Institute of Earth's Cryosphere, Tyum. SC of SB RAS,
Federal Research Center, Tyumen, Russia

ABSTRACT

During the decay of radioactive radium E, electrons with a continuous spectrum of velocities are emitted. The average energy measured with a calorimeter is 0.36 MeV. Based on the dependence of mass on velocity accepted in the Theory of Relativity, W. Pauli calculated the kinetic energy of the electron and obtained a value of 1.16 MeV. For explaining the excess energy of 0.8 MeV, a new particle, neutrino, was postulated. In the present study, we show that the experimental laws of electromagnetism were misinterpreted in the Theory of Relativity. Using the correct laws, we have derived the right expression for the force exerted on a moving charged particle. This expression depends on the distance from the acting object and on the particle velocity. According to the new expression for the interaction force, the particle mass suffers no change. Therefore, there is no reason to introduce a neutrino. As a result of the electromagnetic interaction, particles move along other trajectories that were not known previously. Therefore, the wrong interpretation of particle motions has led researchers to the introduction of fictitious particles that now in large quantities inhabit the imaginary microcosm. It is necessary to reconsider the erroneous postulates on the basis of real interaction forces. This revision must be started from Rutherford experiments without invoking the Theory of Relativity and Quantum Mechanics.

Keywords: Neutrino, β-radiation, energy, charges, motion, force, trajectories.

INTRODUCTION

The decay of a number of radioactive elements is accompanied with β-radiation in a continuous spectrum, i.e. with the emission of electrons with a continuous velocity distribution. This phenomenon contradicted the concept of the discreteness of energy levels in atoms. In the 1920s, it was deduced from the developing quantum mechanics that the energy spectrum of particles emitted during the decay of nuclei had to be discrete. The energy of particles must be corresponding to the difference between energy levels. Therefore, for the followers of quantum theory the continuous spectrum of emitted electrons was a serious obstacle to all quantum mechanical constructions [1, 2].

In order to save quantum mechanics, on December 4, 1930 W. Pauli writes a letter to the participants of the physics conference in Tübingen. In that letter, he puts forward a hypothesis that β-decay is accompanied by the emission of a neutral particle, which takes away so much of the decay energy that the sum of the energy of the newly introduced particle and the energy of the electron remains unchanged. This particle was later given the name neutrino. Initially, this hypothesis, due to its absurdity, was rejected, but with time it was fitted by the supporters of quantum mechanics into the modern picture of the microworld.

CONTINUOUS B-DECAY SPECTRUM

Apparently, it was A.H. Bucherer who for the first time experimentally identified the continuous spectrum of electron velocities during the radioactive decay [3]. The central element of the Bucherer arrangement (Figure 1a) was a flat circular capacitor 8 cm in diameter (Figure 1b). The spacing between the capacitor plates was defined by 4 quartz flakes with a diameter of 5 mm and a thickness of 0.25075 mm. A 0.5-mm pellet of radioactive radium fluoride was placed at the center of the capacitor. The capacitor was located in an 8-cm high brass cylindrical box 16 cm in diameter, which was placed in a uniform magnetic field of strength H. Inside the box, photographic film 2, stretching along the cylindrical surface of the box, was located (Figure 1b). The radium pellet emitted β-rays in all possible directions. Those electrons passed through the narrow slot of the capacitor, where the action of the electric field E due to the capacitor and the action of the magnetic field H, perpendicular to it, were mutually compensated.

As it is evident from Figure 1b, the negative electron will be acted upon inside the capacitor by the upward force due to the capacitor and by the downward force due to the magnetic system. Therefore, only those particles, for which the magnetic and electric forces turn out to be mutually balanced, will leave the centrally located radioactive source. After leaving the capacitor, the "compensated electrons" are entering the only one magnetic field, experienced a deflection in it, reached the photographic film, and produced blackening on the film.

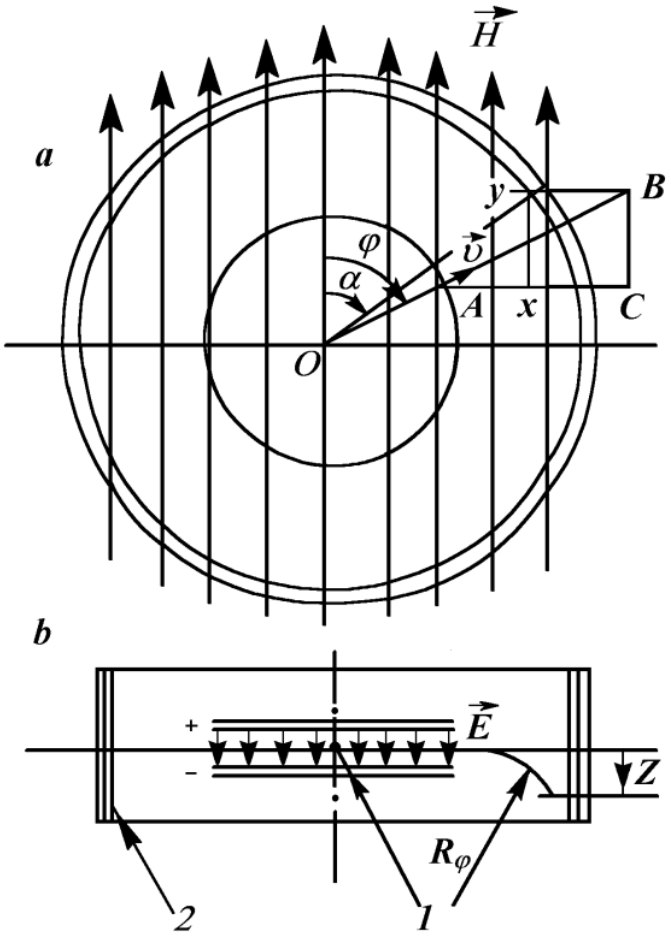

Figure 1. Schematic of the Bucherer experiment [3]:

a – view along the central axis of the capacitor; *b* – view on the diametrical section of the capacitor. *1* – source of β-rays; 2 – photographic film.

The angle φ is reckoned on the film from the direction of the magnetic field H (Figure 1a). In the direction $\varphi = \pi/2$, the electrons fly out of the capacitor at the lowest velocity. Therefore, in the magnetic field they acquire the largest deviation (Figure 2). The more the angle φ differs from π/2, the faster the electrons fly out of the capacitor, and the less they become deflected by the magnetic field. The larger the angle φ differs from π/2, the faster the electrons escape from the capacitor and the less they become deflected by the magnetic field. At angle $\varphi = \arcsin\frac{E}{H}$, electrons fly out of the capacitor at a velocity approaching the speed of light *c*. As it is seen from Figure 2, such particles are not deflected in the magnetic field. The line obtained on the photographic film thus represents the spectrum of electron velocities during the decay of radioactive radium. With the polarity of the fields *E* and *H* having been reversed, a line appears in the upper half-plane. The photographic film also shows a horizontal line produced by γ-radiation and fast electrons. A characteristic feature of the electron spectrum line is that this line intersects the horizontal line at an acute angle.

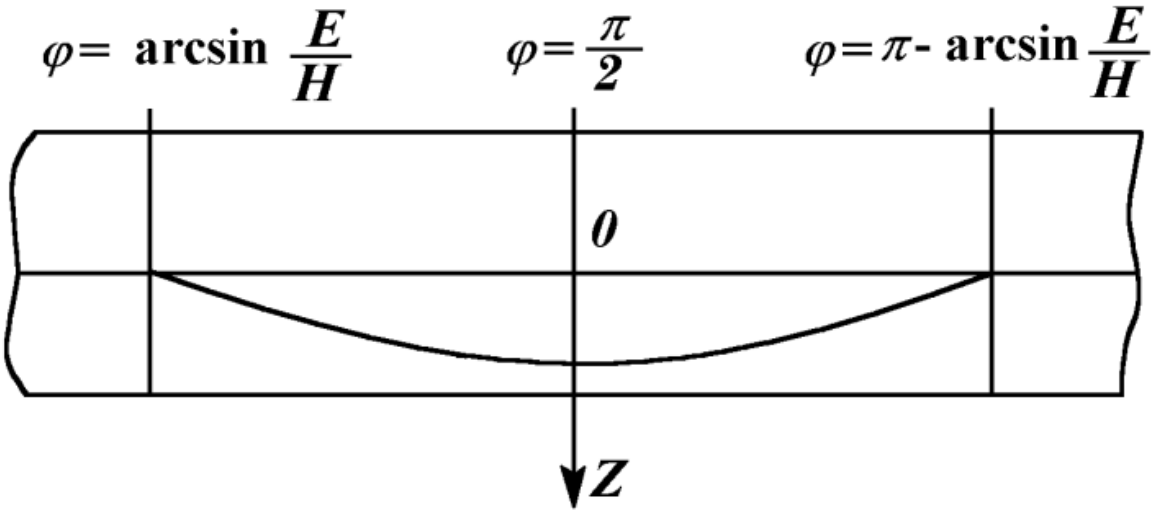

Figure 2. Curve of deviation of the electrons with different velocities on the photographic film in Bucherer's experiments [3].

A study of the continuous spectrum of the β-radiation of radioactive RaE, or bismuth ($^{210}Bi_{83}$), was performed in 1927 by C.D. Ellis and W.A. Wooster [4]. At the beginning of their article, the authors cite the results of a study by Mr. Madgwick of the Cavendish Laboratory, concerning the energy distribution of emitted electrons. Those measurements were carried out using an ionization chamber. The distribution curve of electrons exhibits a smooth behavior with a maximum at 0.30 MeV energy. In this case, the electron energy varies from 0.040 to 1.050 MeV, with the average value being W_m = 0.39 MeV. The aim of the work by C.D. Ellis and W.A. Wooster was the determination of the total energy of electrons using a calorimeter. As a result of several series of experiments, a calorimetric mean electron energy W_{cm} = 0.35±0.04 MeV was obtained. That is, the energy that was determined using the calorimeter proved to be coincident within the experimental error with the mean energy W_m.

In a later paper by W.W. Buechner and R.J. van de Graaff [5], it was confirmed that the calorimetrically determined energy of electrons corresponded to their energy spectrum. Therefore, according to the authors, there were no reasons for the occurrence of additional energy losses due to emission of any other radiation, including neutrinos.

Thus, those experiments showed a continuous spectrum of β-radiation, with the calorimetrically measured energy corresponding to this spectrum. As already noted, the continuous spectrum was in contradictions to quantum-mechanical concepts, and the measured energies did not agree with the electron energies calculated using the Theory of Relativity. For example, W. Pauli has calculated the kinetic energy of an electron using the relativistic formula [2, 6]:

$$W_{cr} = m_e c^2 (1/(1-\beta^2) - 1), \quad (1)$$

- where m_e is the electron mass;
- c is the speed of light;
- $\beta = v/c$ is the electron velocity reduced by the speed of light,
- and obtained the following value of W_r: W_r = 1.16 MeV.

This value was in excess of the experimental value of 0.36 MeV by 0.8 MeV. It was proposed to assign the excess energy of 0.8 MeV to neutrino. It was assumed that during the decay of each atom, the neutrino, together with the electron, took away the energy of 1.16 MeV. Since no other particles were detected during the decay of an atom, the properties of neutrino as a particle without mass, moving at the speed of light and not interacting with the matter, were accepted. The introduction of such a particle led to many contradictions. For example, since the electrons had different velocities and energies, neutrinos would also have different energies for the decay of each atom to be accompanied by the release of the same energy. Meanwhile, all these contradictions were ignored. The energies of all nuclear reactions have been experimentally measured. Neutrino energy was added to them, and then this energy was immediately subtracted as neutrinos disappear without a trace.

THE INFLUENCE OF A MOVING CHARGE ON A STATIONARY CHARGE

Neutrinos and many other particles were invented by theoretical physicists when considering various microcosm models based on the change of the mass of a moving particle in the Theory of Relativity (TR):

$$m = m_0/(1-\beta^2), \quad (2)$$

where m_0 is the mass of the particle, which in the TR is called the rest mass.
The above relativistic expression (1) for the kinetic energy of particle is due to the change of mass (2). The hypothesis about the change of the mass of two charged particles moving relative to each other was introduced into the Theory of Relativity to explain the interaction of two particles.

However, the Theory of Relativity is erroneous [8–10]. The interaction of two charged particles,

q_i and q_k (Figure 3), is determined by the force (3), which depends on the velocity $\vec{v}_{ik}$ and on the distance $\vec{r}_{ik}$ between them [8, 9, 11]:

$$\vec{F}_{ik} = \frac{q_i q_k \left(1-\beta_{ik}^2\right)\vec{r}_{ik}}{\varepsilon\left\{r_{ik}^{\ 2} - [\vec{\beta}_{ik}\times\vec{r}_{ik}]^2\right\}^{3/2}}, \tag{3}$$

- where $\vec{r}_{ik}$ is the radius-vector drawn from particle q_k to particle q_i;
- $\vec{v}_{ik}$ is the velocity of particle q_k relative to particle q_i;
- $\vec{\beta}_{ik} = \vec{v}_{ik}/c_1$ is the reduced velocity;
- $c_1 = c/\sqrt{\mu\varepsilon}$ is the speed of light in the medium filling the space between the particles;
- ε and μ are the dielectric permeability and magnetic penetrability of the medium;
- $[\vec{\beta}_{ik}\times\vec{r}_{ik}]$ is the vector product of $\vec{\beta}_{ik}$ and $\vec{r}_{ik}$.

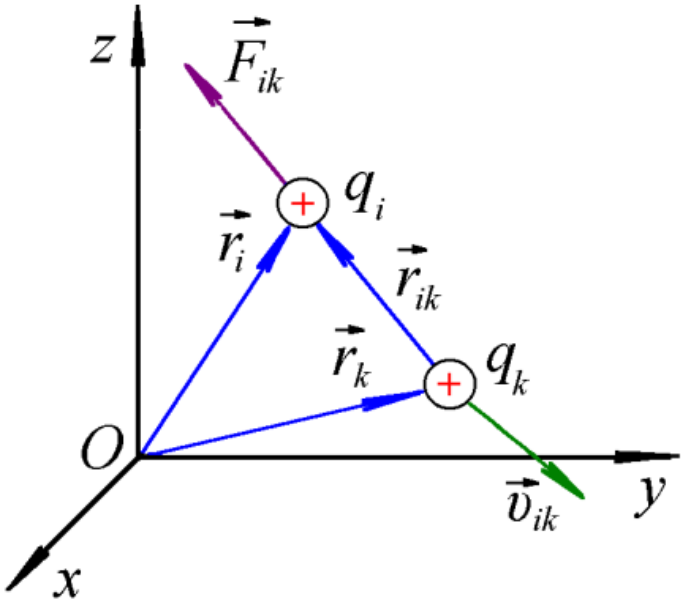

Figure 3. The force $\vec{F}_{ik}$ exerted on the charged particle q_i from the side of the charged particle q_k, moving with a velocity $\vec{v}_{ik}$ relative to the particle q_i.

Since the force (3) changes with a change in particle velocity, the change in particle mass accepted in the TR does not exist. Neither exist all imaginary particles [12].

The Theory of Relativity always treats the interaction of two particles. In reality, not two, but several particles interact simultaneously. Formula (3) expresses the force exerted by a *k*–th particle on an *i*–th particle. In this case, each of the *i*–th particles is acted upon by the remaining *k*-particles. Therefore, in order to describe the real interaction within the Theory of Relativity, one has to introduce as many changes of mass, time, and distance related with the particle *i* as there exist *k*–th particles. These changes must occur to the particle *i* simultaneously. This shows how absurd the Theory of Relativity is. This is first. Second, this inference also shows that the calculation of the interactions between charged particles in the Theory of Relativity is incorrect.

DETERMINATION OF THE FORCE OF ACTION OF A MOVING CHARGE ON A STATIONARY ONE

Expression (3) for the force of action of a particle with charge q_2 on a particle with charge q_1 was obtained based on the experimental laws of electromagnetism [9, 13–14]. Like Figure 3, Figure 4 illustrates the interaction between particles q_1 and q_2 but, here, under the stationary particle q_i we understand the particle q_1, and under the particle q_k, the moving particle q_2.

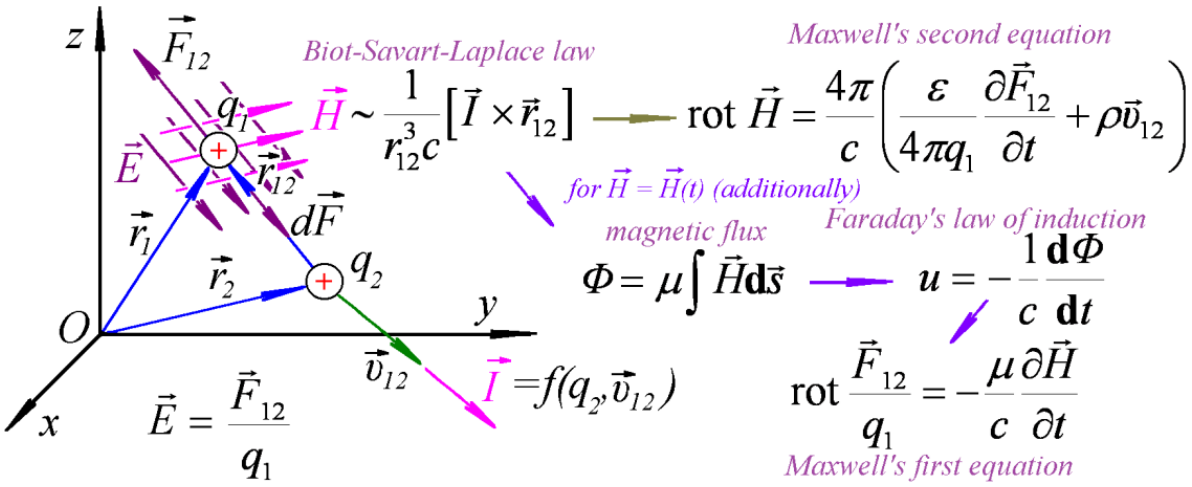

Figure 4. The mechanism of the electromagnetic action of a particle with charge q_2, moving at a velocity $\vec{v}_{12}$, on a particle with charge q_1.

The motion of the particle q_2 is equivalent to a current $\vec{I}$ that creates a magnetic field $\vec{H}$. The alternating magnetic field $\vec{H}(t)$ creates an electric field $\vec{E}$, thus resulting in the emergence of an additional force $d\vec{F}$. Those processes are expressed in the form of the experimental Biot-Savart-Laplace and Faraday laws, whose differential form gives respectively the second and first Maxwell equations.

The particle q_2 moves at the velocity $\vec{v} = \vec{v}_{12}$ relative to the particle q_1 (see Figure 4). Therefore, the movement of particle q_2 is identical to a current I defined as the rate of charge change $I = \frac{dq_2}{dt}$. In order to pass to differential quantities, one has to distribute the charge q_2 over space. For this purpose, the charge density ρ is introduced, which is defined by the expression

$$q_2 = \int_V \rho dV\,, \tag{4}$$

- where V is the volume occupied by the charge q_2.

After differentiating the charge q_2, we obtain an expression for the current $\vec{I}$, which can be conventionally written as $\vec{I} = f(q_2, \vec{v}_{12})$ (Figure 4). In accordance with the Biot-Savart-Laplace law, this current creates a magnetic field

$$\vec{H} = \frac{1}{r_{12}^3 c}\left[\vec{I} \times \vec{r}_{12}\right] \tag{5}$$

with strength H at the location of the first particle. In Figure 4 this magnetic field is shown with orange arrows.

The magnetic field is also characterized by the magnetic flux Φ. Since the second particle q_2 is moving, the field H and the flux Φ appear as variable quantities. According to the Faraday law of induction

$$u = -\frac{1}{c}\frac{d\Phi}{dt}, \tag{6}$$

the alternating magnetic field H at the location of the first particle creates an electric field with strength E, whose potential difference u is determined by the rate of change of the magnetic flux Φ. In Figure 4, the electric field with strength E is shown with brown arrows.

According to the definition of the field strength E, this quantity is the force of action exerted on the first particle with its charge being equal to unity, i.e. $E = F_{12}/q_1$. It was shown in [8, 9] that the Biot-Savart-Laplace law in differential form gives the second Maxwell equation

$$\text{rot}\ \vec{H} = \frac{4\pi}{c}\left(\frac{\varepsilon}{4\pi q_2}\frac{\partial \vec{F}_{12}}{\partial t} + \rho\vec{v}\right), \tag{7}$$

and the Faraday law gives the first Maxwell equation

$$\text{rot}\ \frac{\vec{F}_{12}}{q_2} = -\frac{\mu}{c}\frac{\partial \vec{H}}{\partial t}. \tag{8}$$

Eliminating the strength H from these equations, we obtain the following differential equation for the force exerted by the moving charge q_2 on the stationary charge q_1:

$$\frac{\partial^2 \vec{F}_{12}}{\partial x^2} + \frac{\partial^2 \vec{F}_{12}}{\partial y^2} + \frac{\partial^2 \vec{F}_{12}}{\partial z^2} - \frac{1}{c_1^2}\frac{\partial^2 \vec{F}_{12}}{\partial t^2} = \frac{4\pi q_1}{\varepsilon}\left[\frac{1}{c_1^2}\frac{\partial\left(\rho \vec{v}_{12}\right)}{\partial t} + \text{grad}\ \rho\right], \tag{9}$$

where ρ is the spatially distributed density of charge q_2.

As a result of solving Eq. (9) for a point charge q_2, expression (3) for the force was obtained [13, 14]. The solution of equation (9) is a significant achievement in mathematics. This solution was obtained by the present author in 1968. It should be borne in mind that in this case the indices in expression (3) are as follows: $i = 1$, $k = 2$.

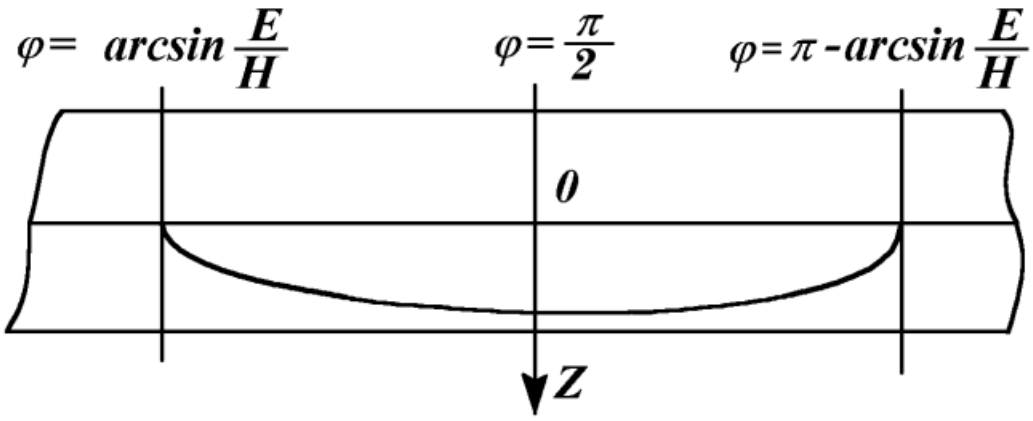

Figure 5. The deflection of electrons moving at different velocities in a capacitor as calculated in the article by K.N. Shaposhnikov [7] according to the Theory of Relativity.

With the help of force (3), the interactions of a charged moving particle with charged bodies of various shapes, a current-carrying conductor, and magnets were analyzed [8]. The theory of accelerators for elementary particle was developed. It is shown that calculations using force (3) are more accurate than the calculations based on the Theory of Relativity.

For example, in the experiment by A.H. Bucherer [5] (see Figure 1), for the electron velocity approaching the speed of light it was found that the Theory of Relativity yields incorrect results. In 1919, in his article [7] K.N. Shaposhnikov showed that for particles whose velocity approached the speed of light, the particle velocity distribution line intersects the horizontal line at the right angle (Figure 5). On the contrary, when the calculations are carried out using force (3) [13, 14], this line intersects the horizontal line at an acute angle, like it is shown in Figure 2. Therefore, the calculations of the interactions between charged particles in the Theory of Relativity are approximate; and at velocities approaching the speed of light they become incorrect.

NEW PARTICLE TRAJECTORIES

As a result of the action of one on another particle according to the Coulomb law, the trajectory of the latter particle can be an ellipse, a parabola, or a hyperbola. These trajectories were used in the analysis of inter-particle interactions. This analysis has led researchers to the knowledge about the occurrence of many different particles in the microcosm. However, when particles interact with one another according to law (3), the trajectories will be different.

We solved the two-particle interaction problem using the force (3) [13, 14]. The trajectory equation is obtained in the following dimensionless form:

$$\varphi = \int \frac{d\bar{R}}{\bar{R}^2 \bar{v}_r} \tag{10}$$

- where $\bar{v}_r = v_r / v_p$ is the dimensionless radial velocity of particle q_1 relative to particle q_2, which is determined by the expression

$$\bar{v}_r = \frac{1}{\beta_p}\sqrt{1-\frac{\beta_p^2}{\bar{R}^2}-\left(1-\beta_p^2\right)\exp\left[2\alpha_1\beta_p^2\left[\frac{1}{\sqrt{\bar{R}^2-\beta_p^2}}-\frac{1}{\sqrt{1-\beta_p^2}}\right]\right]}, \quad (11)$$

- where $\bar{R} = r/R_p$ is the dimensionless distance from particle q_2 to particle q_1;
- $\beta_p = v_p/c_1$ is the reduced velocity of particle q_1 at pericenter (under pericenter, we understand the shortest distance between the particles on their trajectory);
- R_p and v_p are the pericenter radius of the orbit and the particle velocity at the pericenter;
- $\alpha_1 = \mu_1/\left(R_p v_p^2\right)$ is the trajectory parameter;
- $\mu_1 = \frac{q_1 q_2\left(m_1+m_2\right)}{\varepsilon m_1 m_2}$ is the electromagnetic interaction constant;
- m_1 and m_2 are the masses of particles q_1 and q_2, respectively.

The trajectory equation (10) is written in the polar coordinate system (r, φ). At the center of this system, the particle q_2 is located, and the polar angle φ is measured from the pericenter. It is evident from expressions (10) and (11) that the dimensionless trajectories are determined by two parameters, α_1 and β_p. In the case of attraction, i.e. with a positive charge at the central particle q_2 and a negative charge at the particle q_1, for the trajectory parameter we have $\alpha_1 < 0$. In the case of the inter-particle interaction proceeding according to the Coulomb law, the trajectories depend on the parameter α_1 only [8, 9] and, depending on the magnitude of that parameter, those trajectories will be either elliptical orbits ($-1 \le \alpha_1 < -0.5$) or hyperbolic trajectories ($-0.5 < \alpha_1 < 0$). At α_1 = -1, the orbit is a circle, and at α_1 = -0.5 the trajectory is a parabola. It should be noted that Coulomb orbits result from equation (10) and formula (11) with $\beta_p \to 0$. Therefore, these expressions appear as generalized equations for the trajectories of electromagnetically interacting particles, and they are valid both for the Coulomb and electromagnetic interactions of particles.

Expressions (10) and (11) define a wide spectrum of trajectories [15–17]. In Figure 6, this spectrum it shown for varied parameters α_1 and β_p. For example, at α_1 = -0.8 and β_p = 0.3 the point represents the positively charged particle q_2. The negatively charged particle q_1 is located at the right of the horizontal axis at the orbit pericenter, whose dimensionless radius is $\bar{R}_p$ = 1. The particle moves to the left along a quasi-elliptical orbit and reaches the apocenter, or the most distant point of the orbit, with dimensionless radius $\bar{R}_a$ = 1.54. In this case, the polar angle is φ_a = 3.243, i.e. this angle is greater than π, so that an angular displacement of the apocenter occurs. During the second half-period, the same angular displacement will occur as well and, as a result, the pericenter will become shifted over the period by the double angle $2\cdot(\varphi_a - \pi)$. At this value of the trajectory parameter, α_1 = -0.8, the apocenter radius of the Coulomb orbit is $\bar{R}_a$ = 1.667, and the polar angle is $\varphi_a = \pi$.

At a higher velocity of the particle, β_p = 0.5, and at the same trajectory parameter α_1 = -0.8 (see Figure 6), we have $\bar{R}_a$ = 1.27 and φ_a = 3.601, i.e. here the apocenter radius has decreased even

more, and the displacement of the pericenter has further increased in comparison with the Coulomb trajectory. As the particle velocity further increases, the apocenter radius $\overline{R}_a$ approaches unity, the angle φ_a increases, and the orbit becomes a circle. On line *1* or on line C, the orbits become either circles or trajectories turning into circles.

As the absolute value of α_1 decreases, the orbits become more elongated; and at α_1 = -0.5 they open, i.e. the orbit becomes a parabola. Along the parabola, the particle moves away from the attracting center with a velocity equal at infinity to zero. On line 2 or on line *P*, there are quasi-parabolic trajectories.

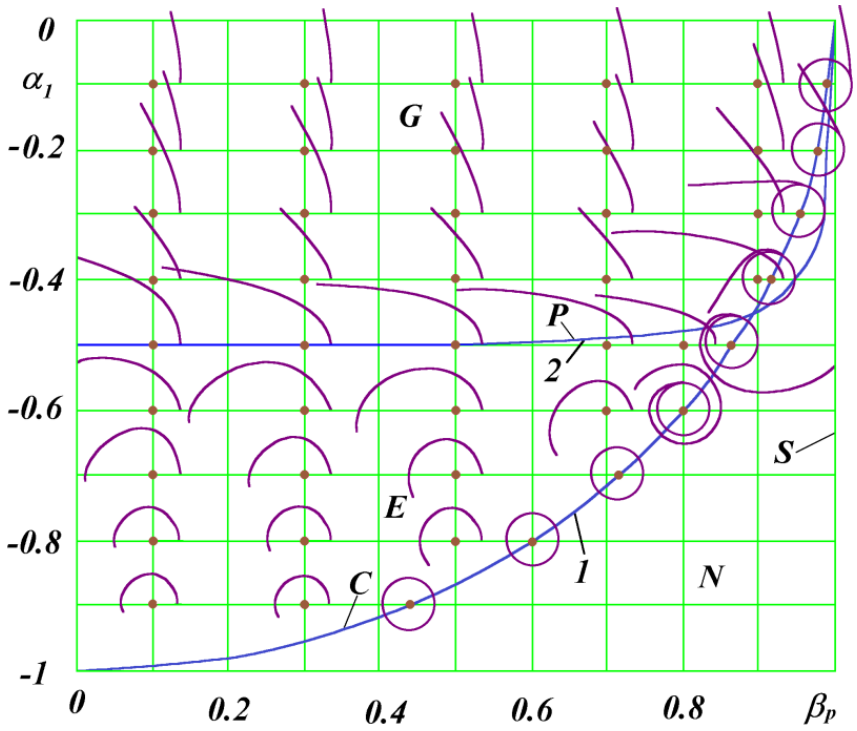

Figure 6. Types of trajectories for the interaction of two particles according to law (3) depending on the values of α_1 and β_p:

G – quasi-hyperbolic; *P* – quasi-parabolic; *E* – quasi-elliptical trajectories; *C* are the limit trajectories passing into circles; *S* – at light speed at the pericenter; *N* – no trajectories; $\alpha_1 = \mu_1/\left(R_p v_p^2\right)$ is the trajectory parameter; $\mu_1 = \frac{q_1 q_2 (m_1 + m_2)}{\varepsilon m_1 m_2}$ is the interaction constant; v_p is the particle velocity at pericenter with radius R_p; $\beta_p = v_p/c_1$; c_1 is the speed of light in the medium with dielectric permeability ε and magnetic penetrability μ.

With a further decrease in the absolute value of α_1, the orbits become quasi-hyperbolic, i.e. the particle moves away from the attracting center with a certain velocity at infinity. As evident from Figure 6, as the velocity β_p increases, the trajectory at infinity approaches the horizontal axis. This means that the angle between the asymptote and the horizontal line decreases, and it may even become negative.

TRAJECTORIES AT LIGHT SPEED AT THE PERICENTER

On the line *S* (Figure 6), there are trajectories with a velocity at pericenter tending to the speed of light, i.e. at $\beta_p \to 1$. Here, there is a wide range of trajectories exhibiting very unusual particle motions [8, 9]. In this case, parameters of the attracting center are such that, as a result of the Coulomb interaction, the center imparts the infinitely distant particle the speed of light on its surface. In a similar case with gravitational interaction, the attracting center was called the Black Hole. According to law (3), in the case of electromagnetic interaction the particles move freely in such a "black hole". Therefore, their trajectories for $\beta_p \to 1$ were called in [8, 9] intra-hole trajectories, or trajectories inside the "black hole". Here, under the "black hole" we mean not some new natural object, but an attracting center with certain proportions of parameters. Particles can freely enter it and freely leave it. Those trajectories can explain many particle interaction processes proceeding in nuclei.

The previous trajectories were obtained by numerical integration of equation (10) at the pericenter ($R_0 = R_p$). With the velocity at pericenter tending to c_1, there arises a double uncertainty at this point. That is why in this case the integration of the equations began at an intermediate point $R_0 > R_p$, and the integration in our calculations proceeded from this point in two directions: towards the pericenter and towards the remote points of the trajectory. For each trajectory, at the starting point R_0 the radial velocity υ_{r0} and the transversal velocity υ_{t0}, perpendicular to the radial velocity, were specified so that the particle velocity at pericenter υ_p tended to the speed of light c_1. With variation of governing parameters, the whole spectrum of trajectories was obtained in [8, 9]. Here, we will analyze only some of those trajectories [10].

Figure 7 shows the trajectories for the trajectory parameter α_1 = -0.498 and for the reduced transversal velocity β_{t0} = 0.93. The properties of the trajectory equation (10) determine the equality $R_0/R_p = 1/\beta_{t0}$. The trajectories in Figure 7 differ in radial velocity. For trajectory *1*, at a low reduced radial velocity of β_{r0} = 0.1, the apocenter angle is $\varphi_a° = 59.8°$, so that the particle makes in one period a little less than a third of a revolution around the other particle. In three periods, the particle makes almost a complete revolution, without 1.2°. At the pericenter points, the particle moves almost at the speed of light, while at the apocenter points its velocity decreases, and the particle slightly gets away from the center by a distance of R_a/R_p = 1.103, as a result, the particle moves with small jumps from the circle of radius R_p.

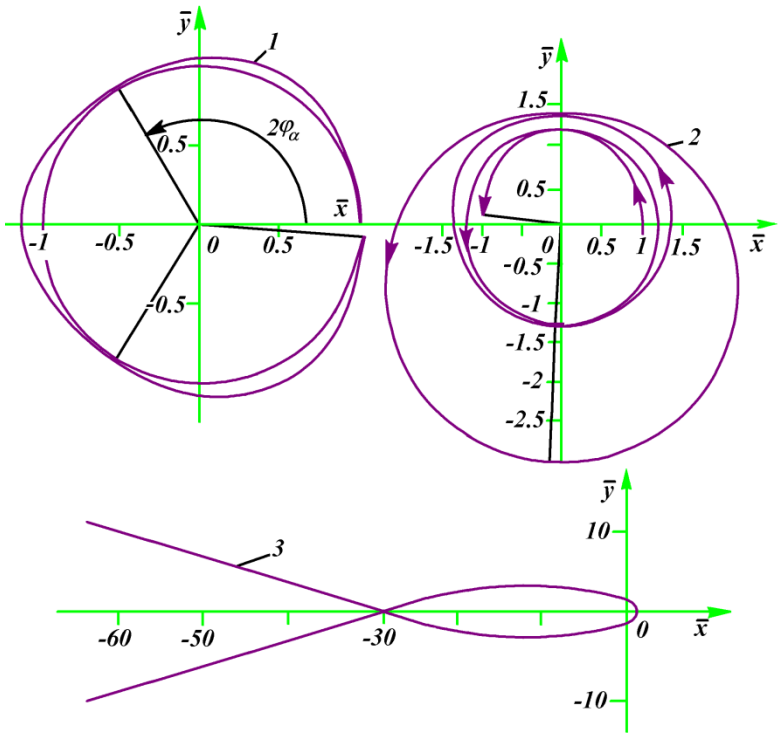

Figure 7. Trajectories at light speed in the pericenter:

α_1 = -0.498, $\beta_p \to 1$; β_{t0} = 0.93, $R_0/R_p = 1/\beta_{t0}$; *1* – β_{r0} = 0.1, *2* – β_{r0} = 0.129, *3* – β_{r0} = 0.2; quasi-elliptic (*1*, *2*) and quasi-hyperbolic (*3*); for one period (*2*, *3*), for three periods (*1*); coordinate system: $\bar{x} = x/R_p, \bar{y} = y/R_p$.

At a higher reduced radial velocity of β_{r0} = 0.129 in trajectory *2*, the apocenter angle is φ_a° = 626.8°, i.e. during almost 1.75 revolutions, without 3.2°, the particle continuously moves away from the center to a distance of R_a/R_p = 2.921. During one period it makes almost 3.5 revolutions, without 6.4°. Quasi-elliptic trajectories *1* and *2* are not closed; therefore, over time, the particle can be found at any point in the space bounded by the radius R_a.

At an even higher velocity of β_{r0} = 0.2 in trajectory *3*, the apocenter radius increases and tends to infinity, while the angle φ_a decreases, i.e. the trajectory becomes quasi-hyperbolic. At the pericenter, the particle velocity approaches the speed of light, $\beta_p \to 1$, and at infinity the reduced radial velocity is $\beta_{r\infty}$ = 0.095. This trajectory has a negative angle between the asymptotes, this angle being equal to -18.24°. The trajectory intersects itself at a considerable distance from the attracting center. The asymptotes of this quasi-hyperbola intersect each other not near the pericenter point, but at a distance 30 times exceeding the radius R_p and located in front of this point. When determining the parameters of the attracting center from the characteristics of such a trajectory using the Coulomb law, errors can be made. For example, if we analyze particle tracks in a cloud chamber, then the size of the attracting center may be overestimated, or this interaction of attraction may be misinterpreted as repulsion.

For the trajectories in Figure 7, consider as an example the interaction of a proton and an electron. Here, the pericenter radius will be $R_p = 5.66 \cdot 10^{-15}$ m. According to modern estimates, the proton radius is $R_{pr} = 0.9 \cdot 10^{-15}$ m, and the electron radius is $R_e = 2.8 \cdot 10^{-15}$ m. Therefore, the particles at the pericenter of the trajectories in Figure 7 approach each other to a distance equal to $1.53(R_{pr} + R_e)$.

The quasi-elliptic orbits in Figure 7 explain why during the decay of a neutron, the electrons can be ejected at different velocities, which vary over a wide range and even approach the speed of light. For example, the electron at points of its orbit *2* has such a velocity. With a third particle affecting the electron, the electron will leave its orbit at roughly the same velocity it had at that moment.

CLOSED STABLE ORBITS

For the quasi-elliptical orbits in Figure 6, the pericenter rotates over the period by an excess of the full turn, $\Delta\varphi_p° = 2 \cdot \varphi_a° - 360°$. Therefore, with time this region will become densely hatched by the particle, so that it will then become possible to find the particle at any of the points inside the circle with the apocenter radius R_a. Only in the trajectories with excess $\Delta\varphi_p°$ being a multiple of 360°, i.e.

$$\Delta\varphi_p° = 360°/k, \tag{12}$$

the particle after k periods will follow the same path again. Such an orbit will be closed.

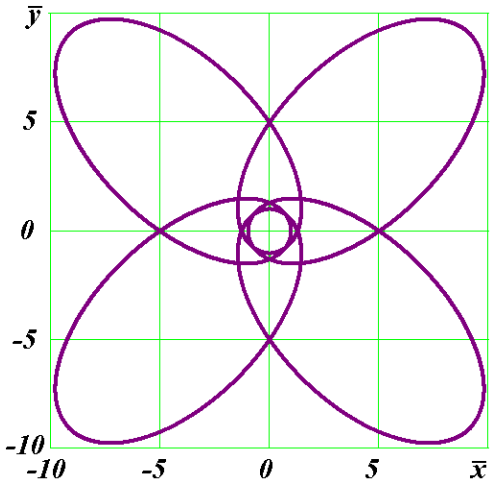

Figure 8. The closed orbit of a particle during 4 motion periods at $\alpha_1 = -0.5$, $\beta_p = 0.8019$, and $2 \cdot \varphi_a° = 450°$.

The path of the particle along the closed orbit is 1800°, i.e. the particle makes 5 revolutions. As applied to the interaction of a proton and an electron, the orbital trajectories approach each other at the pericenter to a distance equal to 2.4 of the sum of their radii.

One such orbit is shown in Figure 8 for $\alpha_1 = -0.5$ and $\beta_p = 0.8019$. Its apocenter radius is $R_a/R_p = 12.8745$, and the apocenter angle is $\varphi_a = 225°$. In a period, the particle travels an angular distance of 450°. In this case, the excess is $\Delta\varphi_p° = 90°$ and, according to relation (12), $k = 4$.

Therefore, after 4 periods the particle will again follow the same path. Along the 4-leaf trajectory, the motion of the particle proceeds without change. The particle repeats this recurring trajectory for $2k{\cdot}\varphi_a° = 1800°$, i.e. here it makes $1800°/360° = 5$ complete revolutions about the central particle.

Like in the case of the trajectory in Figure 8, in the interaction of a proton and an electron with such parameters α_1 and β_p, the pericenter radius is $R_p = 8.77{\cdot}10^{-15}$ m. Therefore, at the pericenter of the trajectory (Figure 8) the proton and the electron will approach each other to a distance equal to $2.4(R_{pr} + R_e)$.

For trajectories *1* and *2* in Figure 7, at light speed at the pericenter one can choose parameters α_1 and β_p such that both the excess $\Delta\varphi_p°$ and the full turn of 360° will have multiple divisors. In those cases, the particle will also travel in a closed orbit.

The term "period" used here applies to the distance between the interacting particles. This distance increases from the minimum one of $\overline{R}_p = 1$ to the maximum one of $\overline{R}_a$, and then it decreases to $\overline{R}_p$ as the angle changes by $2\varphi_a$, where $2\varphi_a$ is the angular period of the function $\overline{R}(\varphi)$. In contrast to the classical case, the particle never returns to the starting point during the period $2\varphi_a$ of the function $\overline{R}(\varphi)$.

If the number π is a multiple of φ_a, then the particle will arrive at the same point in space after making a certain number of periods $2\varphi_a$. From Figure 7, for trajectories *1* and *2*, and from Figure 8 it follows that the angular distance from pericenter to apocenter in this case will be

$$\varphi_a = \pi n + \pi/k, \tag{13}$$

- where $n = 0, 1, 2...$; $k = 1, 2, 3....$

Then, the orbit of the particle will be closed, and it will come to the same point with a period

$$\varphi_c = 2k\varphi_a = 2\pi\,(kn + 1). \tag{14}$$

For example, for the trajectory in Figure 8 we have: $\varphi_a = 225°$, which value, according to formula (13), corresponds to $n = 1$ and $k = 4$. Then, by virtue of formula (14), the period of the closed orbit is $\varphi_c = 10\,\pi$. If for trajectory *1* in Figure 7 an exact equality $\varphi_a = \pi/3$ would be valid instead of $\varphi_a° = 59.8^\circ$, then, according to formula (13), the angle φ_a would be expressed by the coefficients $n = 0$ and $k = 3$, and according to formula (14) the full period would be $\varphi_c = 2\pi$. For trajectory *2* in Figure 7, for $\varphi_a° = (3\pi + \pi/2)57.3^\circ = 630^\circ$ instead of 626.8°, this would correspond to $n = 3$ and $k = 2$, and to the full period $\varphi_c = 14\,\pi$ according to formula (14). In this case, the particle arrives at the starting point in space following two periods of change of the function $\overline{R}(\varphi)$.

The examples of trajectories *1* and *2* in Figure 7 show that the period of a closed orbit of two interacting particles φ_c is capable of varying over a wide range: from 2π to 14π, i.e. by a factor

of 7. In this case, the closed orbits are characterized by integer values of n and k. Since the trajectories and the angle φ_a are determined by the parameters α_1 and β_p, the integer values of n and k correspond to discrete values of α_1 and β_p. These results about the discrete (quantum) parameters of closed orbits are important for understanding atomic physics and the phenomenon of radioactivity.

As noted above, the Coulomb trajectories have been used in the analysis of inter-particle interactions in the microcosm. According to law (3), in the case of electromagnetic interaction the trajectories at velocities $\beta_p < 0.1$ differ little from Coulomb trajectories. As shown in Figure 6 - Figure 8, as the velocity β_p increases, the particle trajectories show transformations. Analysis of results on inter-particle interactions with the help of those trajectories will lead to another microcosm. Therefore, the Special Theory of Relativity must be thrown away and forgotten. It is necessary to investigate the real microworld with the help of new trajectories.

CONCLUSION

The continuous spectrum of β-radiation contradicted quantum mechanics, and the measured energy of β-radiation contradicted the Theory of Relativity, so neutrino particles were invented. However, the continuous spectrum of β-radiation is not canceled by the supposed existence of neutrino particles, and the Theory of Relativity is erroneous, with its calculations of interactions being incorrect. Therefore, there are no reasons for postulating neutrinos. The neutrino does not exist. This is a figment of the imagination of theoretical physicists of the 20th century.

In the 20th century, the Theory of Relativity was created based on the misconception of the interaction of charged particles moving relative to each other. Based on the hypotheses of this erroneous theory, an imaginary four-dimensional world with various transformations in it was constructed. This construction was then extended to the gravitational interaction. In this way, a four-dimensional curvilinear world with various transformations supported by tensor mathematics was built.

Based on these fanciful fantasies, the construction of an imaginary micro- and macrocosm began. For theoretical physicists, there have been enough examples of how the world around them could be populated with chimeras. Yet, the process has begun continuously, unceasingly, and without hesitation.

Throughout this time, there have been many scientists, real explorers of the surrounding world, who opposed those fantasies. But fantasies are sweet to the soul, and they were more attractive to people than sober truths. Therefore, Mainstream has rooted in science, which still continues to populate the world with various chimerical objects like quarks, bosons, Black holes, gravitational waves, Big Bangs, etc [18].

Many neutrino detectors, or neutrino telescopes, have now been built: at FermiLab in the USA, Super-Kamiokande in Japan, ANTARES in the Mediterranean Sea, IceCube in Antarctica, Baikal-GVD at Baikal, etc. Those setups allegedly detect neutrinos. However, when analyzing the reported results, this is not confirmed. For example, Argentine physicist Ricardo Cerezani has

come to the conclusion that these expensive experiments provide super proof of neutrino non-existence [19, 20]. Exactly the same can be said about one of the other macrocosm fantasies, gravitational waves, with the tremendous sophisticated installations for their detection proving the absence of such waves [18].

By the end of their lives, all those dreamers-theorists come to be utterly disappointed by their fantasies [18]. The time has come to put an end to the widespread errors.

All interactions in the microworld are determined by the experimental laws of electromagnetism: Coulomb law, Biot-Savart-Laplace law and Faraday's induction [10], which together give the right expression for the force (3). As a result of electromagnetic interactions, particles move along trajectories that were not known previously. The misinterpretation of particle motions has led scientists to the introduction of fictitious particles that now inhabit the imaginary microcosm. It is necessary to revise physics on the basis of real interaction forces. This revision must begin with Rutherford experiments without invoking the Theory of Relativity and Quantum Mechanics.

All interactions in the macroworld are determined by the Newton experimental law of gravity [10, 21]. The General theory of relativity must be discarded and forgotten. All imaginary constructions and objects must be eliminated from modern cosmology [10, 18]. We need to study and explore the world around us. For this, the researcher needs a lot of time and much effort to spend, but as a result he gets knowledge about the world, which will long serve future generations. It is this knowledge that was obtained in the works by Euclid, Archimedes, Hipparchus, Ptolemy, Copernicus, Galileo, Newton, Coulomb, Laplace, Faraday, Mendeleev and many other thinkers. This knowledge has served us well, and it will continue to serve our descendants.

ACKNOWLEDGMENTS

The data submitted in this work were obtained while performing research activities that have been conducted during three and a half decades at the Institute of Earth's Cryosphere, Tyumen SC of SB RAS, Federal Research Center. In recent years this research project has been carried out under Contract Agreement No. 121041600047-2 with RAS.

References

[1]. *Neutrino*. Wikipedia. 2023. (In Russian). https://ru.wikipedia.org/wiki/%D0%9D%D0%B5%D0%B9%D1%82%D1%80%D0%B8%D0%BD%D0%BE [Accessed: 2023-05-12].

[2]. de Hilster, D., *The Neutrino: Doomed from Inception*. In: Proceedings of the NPA 8, College Park, MD 2011. 2011, p. 148-151. http://www.naturalphilosophy.org/pdf/abstracts/abstracts_6157.pdf [Accessed: 2023-05-12].

[3]. Bucherer, A.H., *Die experimentelle Bestatigung des Relativitats Prinzips*. Annalen der Physik, 1909. Bd 28: p. 513-536. https://doi.org/10.1002/andp.19093330305 [Accessed: 2023-05-12].

[4]. Ellis, C.D., Wooster, W.A., *The Average Energy of Disintegration of Radium E.* Proceedings of the Royal Society A117 (776). London, 1927: p. 109-123. https://doi.org/10.1098/rspa.1927.0168 [Accessed: 2023-05-12].

[5]. Buechner, W.W., *Van de Graaff, R.J., Calorimetric Experiment on the Radiation Losses of 2-MeV Electrons*. Physical Review, 1946. **70** (3 and 4): p. 174-177. https://journals.aps.org/pr/abstract/10.1103/PhysRev.70.174 [Accessed: 2023-05-12].

[6]. Carezani, R.L., *Nuclear-Nuclear Collisions*. 1997. 11p. http://www.naturalphilosophy.org/pdf/abstracts/abstracts_6242.pdf [Accessed: 2023-05-12].

[7]. Shaposhnikov, K.N. *To Kasterin's article: "Sur la nonconcordance do pricipe de relativile d'Einstein"*. Proceedings of the Ivanovo-Voznesensky Polytechnic Institute. 1919; Issue. 1.

[8]. Smulsky, J.J., *The Theory of Interaction*. Novosibirsk: Publishing house of Novosibirsk University, Scientific Publishing Center of United Institute of Geology and Geophysics Siberian Branch of Russian Academy of Sciences. 1999. 294. (In Russian). http://www.ikz.ru/~smulski/TVfulA5_2.pdf [Accessed: 2023-05-12].

[9]. Smulsky, J.J., *The Theory of Interaction*. Ekaterinburg: Cultural Information Bank. 2004. 304. http://www.ikz.ru/~smulski/TVEnA5_2.pdf [Accessed: 2023-05-12].

[10]. Smulsky, J.J., *The Upcoming tasks of Fundamental Science*. M.: Sputnik+ Publishing House. 2019. 134. ISBN 978-5-9973-5228-8. (In Russian). http://www.ikz.ru/~smulski/Papers/InfPrZaFN.pdf [Accessed: 2023-05-12].

[11]. Smulsky, J.J., *The new approach and superlight particle production*. Physics Essays, 1994. Vol. 7, No. 2: p. 153–166. http://www.ikz.ru/~smulski/smul1/English1/FounPhisics/NApSup.pdf [Accessed: 2023-05-12].

[12]. Smulsky, J.J., *New Understanding in Academic Science*. Natural Science, 2019. Vol. 11, No. 3: p. 74-94. DOI: 10.4236/ns.2019.113009. https://www.scirp.org/journal/PaperInformation.aspx?PaperID=91189 [Accessed: 2023-05-12].

[13]. Smulsky, J.J., *The Electromagnetic and Gravitational Actions (The Non-Relativistic Tractates)*. Novosibirsk: "Science" Publisher. 1994. 225. http://www.ikz.ru/~smulski/smul1/English1/FounPhisics/ELGRVZIN.doc [Accessed: 2023-05-12].

[14]. Smulsky, J.J., *Electrodynamics of moving bodies. Determination of forces and calculation of movements*. Saarbrucken, Germany: "Palmarium Academic Publishing". 2014. 324. ISBN 978-3-659-98421-1. (In Russian). http://www.ikz.ru/~smulski/Papers/InfElMvBEn.pdf [Accessed: 2023-05-12].

[15]. Smulsky, J.J., *The trajectories at interaction of two bodies, which depend on relative distance and velocity*. Mathematical Modeling. 1995. Vol. 7, No. 7: p. 111-126. (In Russian). http://www.ikz.ru/~smulski/smul1/Russian1/FounPhisics/TrV2tl.pdf [Accessed: 2023-05-12].

[16]. Smulsky, J.J., *The new fundamental trajectories: Part 1—hyperbolic/elliptic trajectories*. Galilcan Electrodynamics (or “Electromagnetics”). 2002. Vol. 13, No. 2: p. 23–28. http://www.ikz.ru/~smulski/smul1/English1/FounPhisics/NFT.pdf [Accessed: 2023-05-12].

[17]. Smulsky, J.J., *The new fundamental trajectories: Part 2—parabolic/elliptic trajectories*. Galilcan Electrodynamics (or “Electromagnetics”). 2002. Vol. 13, No. 3: p. 47–51. http://www.ikz.ru/~smulski/smul1/English1/FounPhisics/NFT.pdf [Accessed: 2023-05-12].

[18]. Smulsky, J.J., *Dark Matter and Gravitational Waves*. Natural Science. 2021. 13, No. 3: p. 76-87. doi:10.4236/ns.2021.133007. https://www.scirp.org/journal/paperinformation.aspx?paperid=107880 [Accessed: 2023-05-12].

[19]. Carezani, R.L., *Neutrinos at Fermi Lab*. 1997. 3. https://www.naturalphilosophy.org/pdf/abstracts/abstracts_6241.pdf [Accessed: 2023-05-12].

[20]. Carezani, R.L., *Super-Kamiokande: Super-Proof for Neutrino Non-existence*. 1997. 8. https://www.naturalphilosophy.org/pdf/abstracts/abstracts_6243.pdf [Accessed: 2023-05-12].

[21]. Smulsky J.J. Future Space Problems and Their Solutions. New York: Nova Science Publishers; 2018. 269 p. ISBN: 978-1-53613-739-2. http://www.ikz.ru/~smulski/Papers/InfFSPS.pdf [Accessed: 2023-05-12].